

Numerical and experimental study on a large sized water container with a convex curve for shock compaction

Youngkook Kim*, Shigeru Itoh**, and Chai-Bong Lee***†

*Shock Wave and Condensed Matter Research Center, Kumamoto University
2-39-1 Kurokami, Kumamoto City, Kumamoto, 860-8555, Japan

**Okinawa National College of Technology, 905 Henoko, Nago, Okinawa 905-2192, Japan

***†Dept. of Electronics Engineering, Dongseo University
San 69-1, Jurye-2dong, Sasang-gu, Busan 617-716, South Korea
Tel : +82-51-320-1755

†Corresponding address : lcb@gdsu.dongseo.ac.kr

Received : January 10, 2012 Accepted : January 25, 2012

Abstract

A large sized water container with a convex curve for shock compaction was estimated by means of numerical analysis and experiment. The converging effect of reflected waves generated from the wall of water container and its overtaking of the underwater shock wave were confirmed. The magnitude and distribution of shock pressure impacting powders were found to differ depending on position. The arrival time of shock pressure at the top surface of powders also differed depending on position, which was measured at central, 7.5mm and 15mm position from the wall of water container. It was confirmed that the shock pressure was about 11.5 GPa as measured by a manganin stress gauge ; however, this differed slightly from the result of the numerical calculation of 12.8 GPa. For the consolidation of graphite-doped copper (Cu) powders, weak surface bonding was confirmed between graphite and Cu powder particles, and a small crack was observed in the middle position of the compact due to the fast and high shock pressure. However, we successfully obtained a large-sized shock-consolidated graphite-doped Cu bulk with the size of 15mm × 10mm.

Keywords : shock compaction, shockwave, powder

1. Introduction

The shock compaction technique for powders has several unique characteristics such as suppression of grain growth; avoidance of prolonged heat treatment; very short consolidation process within microseconds; strong surface bonding between powder particles; no binder requirement; and high density. For many years, shock compaction techniques using dynamic pressure such as explosive powder compaction¹⁾, gas gun powder compaction²⁾ and related high velocity impact compaction have been developed and studied for commercial applications. In spite of these continued efforts, commercial applications have proven difficult due to both cracking problems and the small size of the compact.

Recently, a shock compaction technique using an underwater shock wave^{3),4)} has attracted considerable attention due to its suitability for compacting powders. This method can control shock pressure using the configuration of a water container, which is a part of the shock compaction device, and sustains longer pressure duration than shock compaction utilizing air⁵⁾. Though studies related to shock compaction using underwater shock wave have been often reported, there has been no mention of the possibility for commercial applications.

In this work, we focused on achieving a compact size suitable for commercial applications by designing a large-sized water container with a convex curve to investigate the magnitude, distribution and propagation of shock

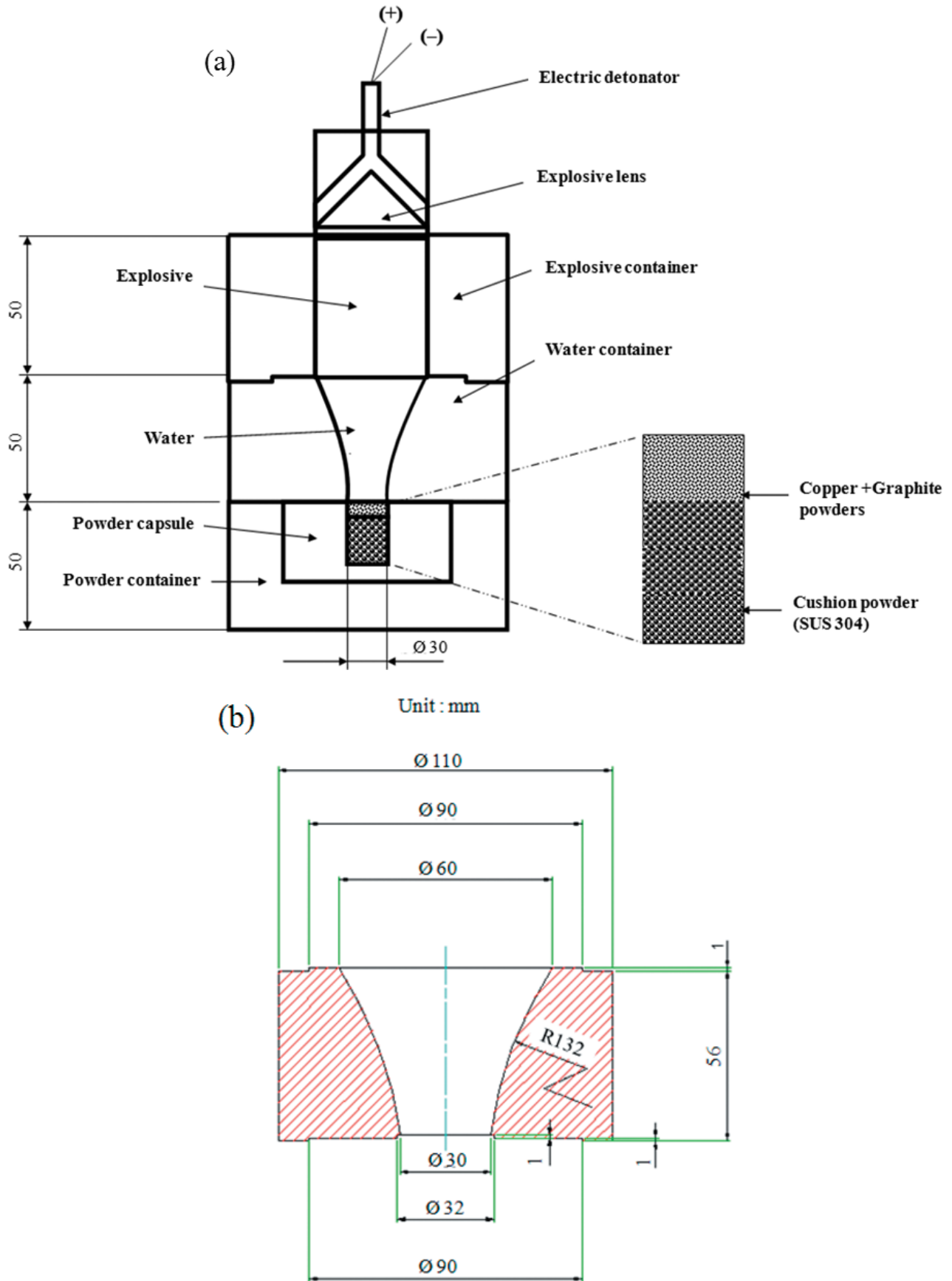


Figure 1 Schematic illustration of (a) shock compaction device and (b) a large sized water container with convex curve.

pressure impacting on the powders using a numerical method and experiments; we then estimated the consolidation of graphite-doped copper (Cu) powders; graphite-doped Cu composite materials are extensively used as sliding bearings and brush applications^(6),7).

2. Experimental set up

The large-sized water container with a convex curve and the compaction device are schematically illustrated in Figure 1. The compaction device consists of an explosive container, water container, powder container and powder

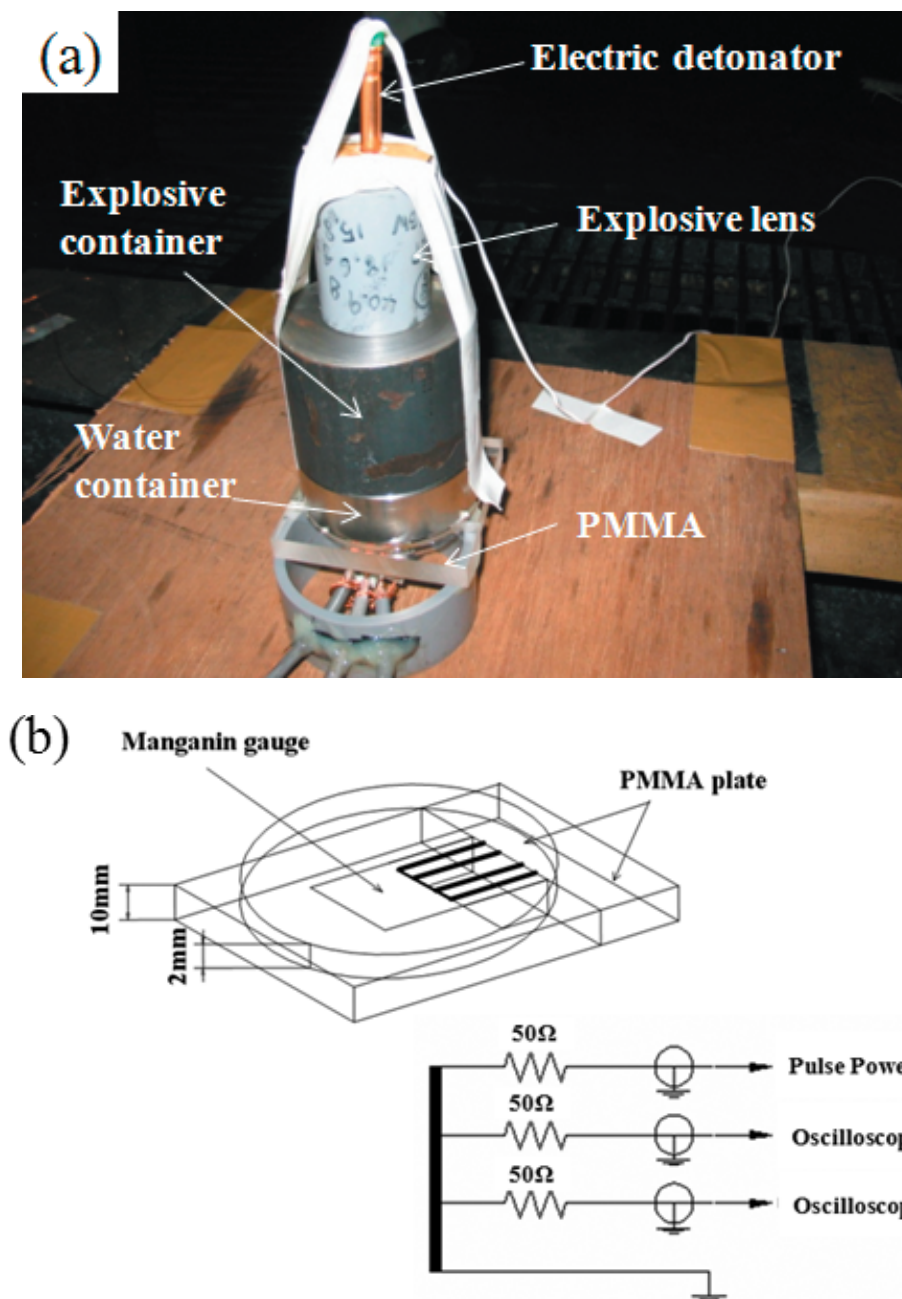


Figure 2 Shock pressure measurement system (a) Photograph of the device (b) Illustration of measurement circuit and manganin stress gauge set up in the PMMA.

capsule. The powder capsule is used for easy sample recovery. The explosive is charged to the explosive container (inner and outer diameters of 70 mm and 110 mm, respectively, and height of 50 mm). The water container is filled with water to transmit the underwater shock waves. For powder consolidation, graphite-doped Cu powders and stainless steel (SUS 304) powders were used. These powders were compacted by a press machine at 50 MPa to the powder capsule. In particular, the SUS 303 powder was used to alleviate the effect of the reflected force.

The generation and propagation behavior of the detonation wave and underwater shock wave were investigated by means of LS-DYNA 3D, a commercial program based on the explicit finite element code. To understand the propagation of these waves, a 2-dimensional photographing method using a high-speed

camera (IMACON 468 Hadland Photonics) was employed. The test device was a 2-dimensional type of water container.

Shock pressure impacting on the powders was measured by a manganin stress gauge (Cu 83.5 %, Mn 11.5 %, Ni 4.4 %) with a thickness of $6\mu\text{m}$ and width of $0.5 \sim 1.0$ mm. The calculation method using the manganin stress gauge was developed by Nakamura and Mashimo⁸⁾. The shock pressure measurement system is shown in Figure 2 (a). The manganin stress gauge is firstly set in the circular, 2 mm-thick PMMA plate and then to the rectangular, 10 mm-thick PMMA plate, as shown in Figure 2 (b); it is then installed below the water container due to the difficulty of directly setting it at the bottom of the water container. Therefore, the shock pressure was measured in the PMMA, at 2 mm from the bottom of the water container.

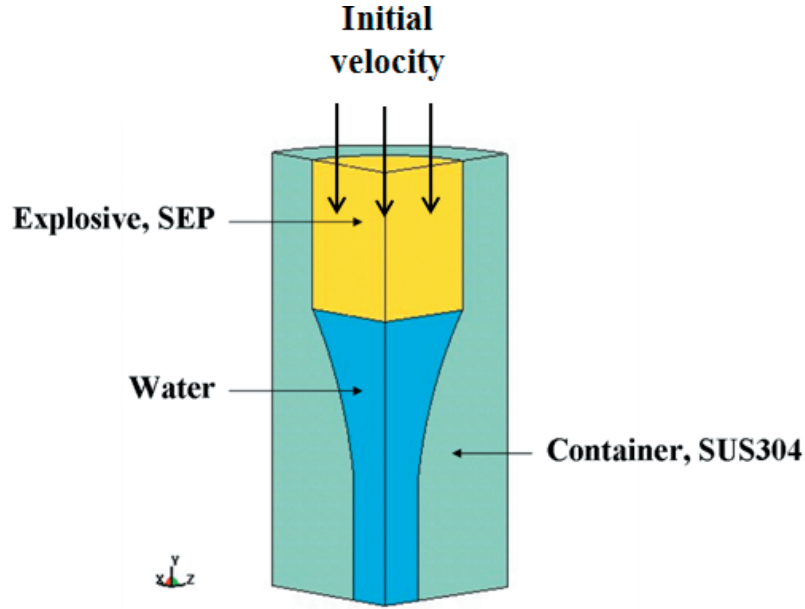


Figure 3 Simplified numerical model of large sized water container with convex curve.

The microstructure of the shock-consolidated graphite-doped Cu bulk was investigated by scanning electron microscope (JCM 5700–JEOL, Japan).

3. Results and discussion

3.1 Numerical analysis

The simplified numerical model is shown in Figure 3. The model was designed as one quarter of a circular cylinder with the initial velocity given as particle velocity of an explosive, 1711 m/s. The model of each material was applied as follows: the elastic–plastic hydrodynamic model is for steel containers, the null model for water and powders. The powders were considered part of the water both because it is difficult to model the physical motion of powder particles and because only the distribution and magnitude of shock pressure impinged on the top surface of powder require confirmation. For the explosive, the JWL equation of state was used, described as follows:

$$P = A \left(1 - \frac{\omega}{R_2 V} \right) \exp(-R_1 V) + B \left(1 - \frac{\omega}{R_2 V} \right) \exp(-R_2 V) + \frac{\omega e}{V} \quad (1)$$

where P is the pressure and V is the ratio of the initial density of explosive to the density of detonation gas products, e is the internal energy. The JWL coefficients, A , B , R_1 , R_2 and ω were determined by the expansion tube test⁹. These parameters are listed in Table 1. For the water and steel containers, the Mie–Grüneisen equation of

state was used and is given as follows. The parameters of water and steel containers are shown in table 2.

$$P = \frac{\eta \rho_0 C_0^2}{(1 - s\eta)} \left(1 - \frac{\Gamma \eta}{2} \right) + \Gamma \rho_0 e \quad (2)$$

where C_0 is the sound velocity, η is the rate of density change of a substance, s is the constant of material and Γ is the Grüneisen parameter, respectively.

The generation and propagation behavior of the underwater shock wave passing through water is shown in Figure 4, which clearly shows that a detonation wave is converted to underwater shock wave and that reflected waves are generated from the wall of the water container. The reflected waves converge in the middle position after overtaking the underwater shock wave. We also confirmed the propagation of the underwater shock wave and reflected waves using a high speed photographing method, which clearly shows that the converging reflected waves are generated from the wall of water container and that the underwater shock wave propagates as a planar wave, as shown in Figure 5. The converging effect allows achievement of a higher shock pressure¹⁰. Figure 6 shows shock pressure profiles obtained from the result of numerical calculation. The maximum peak shock pressure is confirmed as 12.8 GPa at the central position and the position 7.5 mm from the wall –almost the same value at both positions. However, the peak shock pressure at the 15 mm position, i.e. nearest the wall, was much lower than that of the central and 7.5 mm positions. This is caused by the motion of reflected waves, which move to the central axis and converge. The arrival time of peak shock pressure at each position differed slightly, with the fastest near the wall and the 7.5 mm position and central positions later. However, this may be ignored as the difference is very small. Thus, it can be considered that uniform distribution of shock pressure impaction on the powders was achieved. The measured shock pressure by manganin stress gauge was confirmed as approximately 11.5 GPa. Unfortunately, because the gauge was completely

Table 1 JWL coefficients for explosive, SEP.

A[GPa]	B[GPa]	R_1	R_2	ω
364	2.31	4.3	1.00	0.28

Table 2 Mie–Grüneisen parameters of water and container (steel).

	ρ_0 [kg/m ³]	C_0 [m/s]	s	Γ
Water	1000	1489	1.79	1.65
SUS304	7900	4570	1.49	2.17

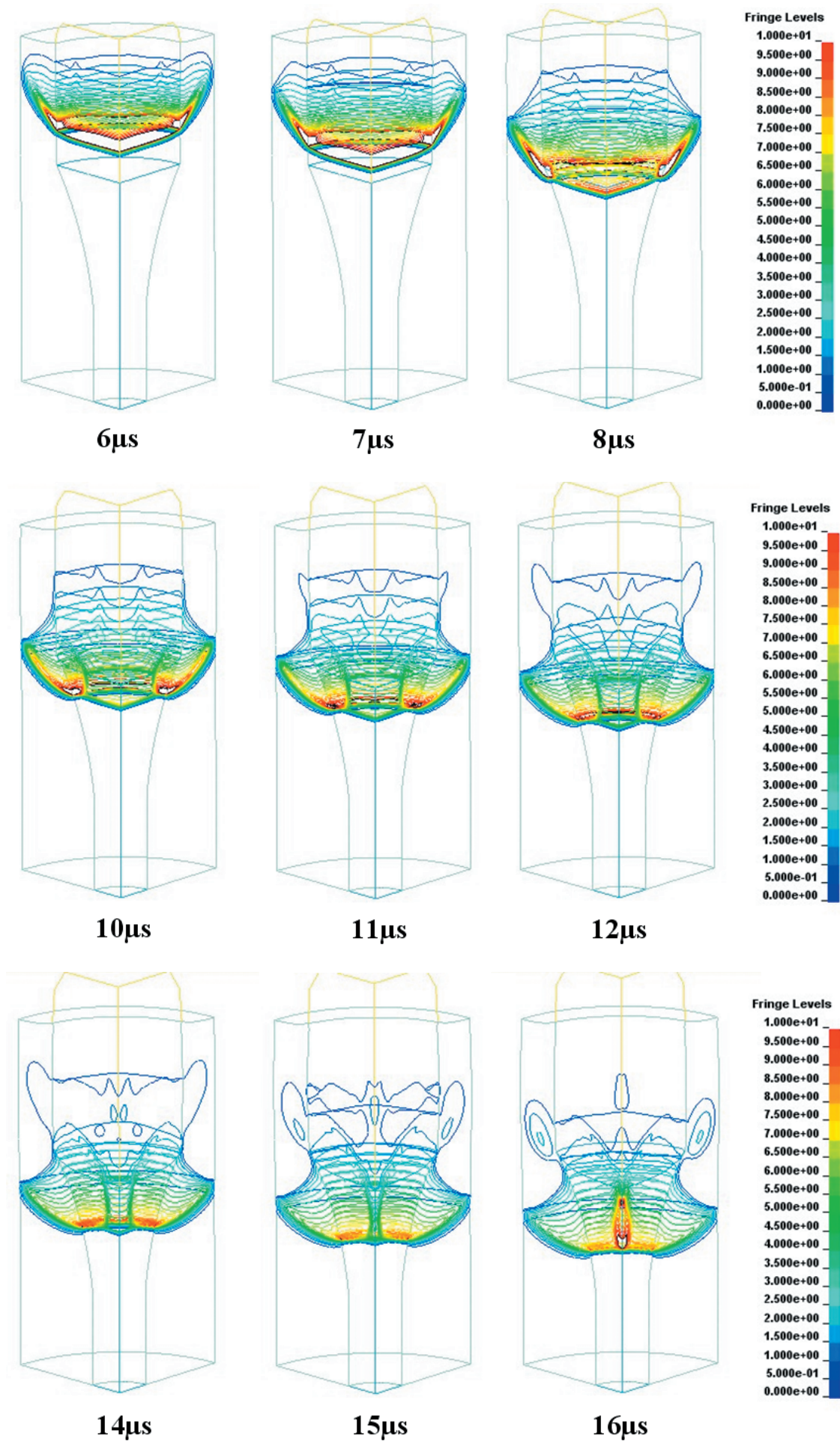


Figure 4 Propagation of underwater shock compaction and reflected wave generated from the wall of water container.

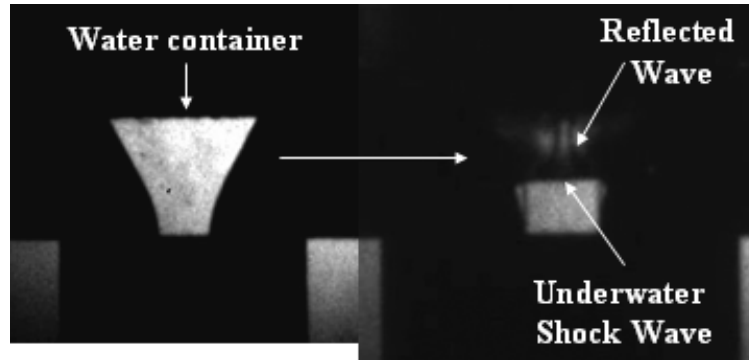


Figure 5 Visualization of propagation behavior of underwater shock wave and reflected waves.

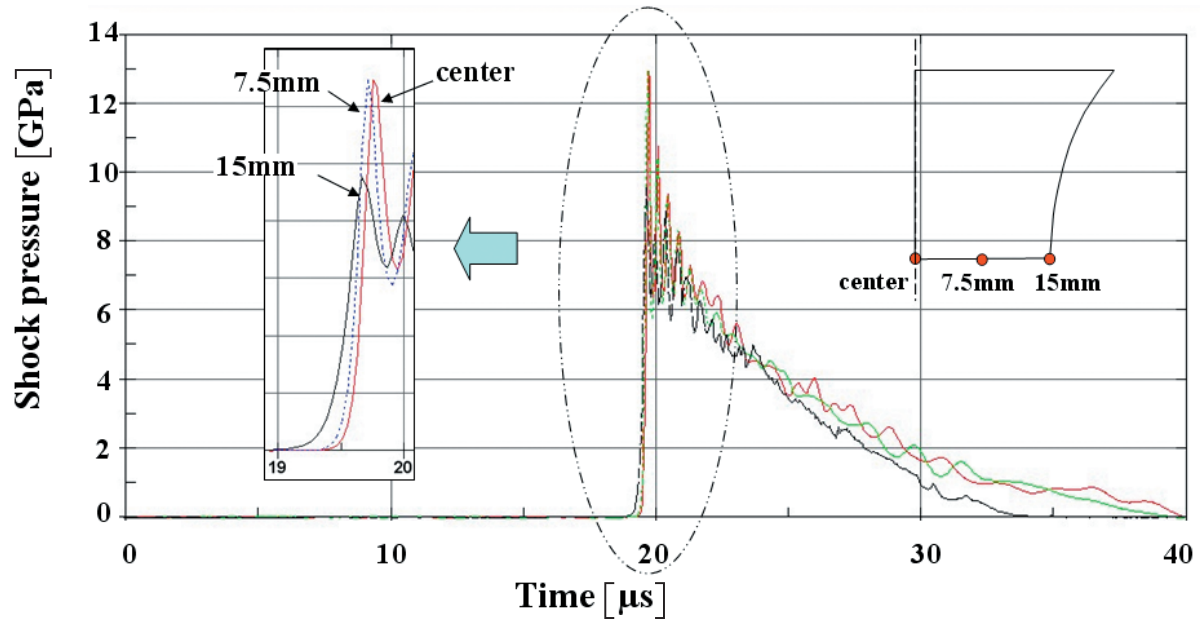


Figure 6 Shock pressure of underwater shock wave at each position (center, 7.5 mm and 15 mm) obtained by numerical calculation.

destroyed upon compaction, the shock pressure presented by the converging effect of reflected waves could not be confirmed. Thus, there the results of the numerical calculation and the real experiment differed slightly.

3.2 Shock compaction

Shock compaction of graphite-doped Cu powders was performed using an underwater shock compaction device with a large-sized water container, which was designed based on the result of numerical analysis. Figure 7 shows photographs of shock-consolidated graphite-doped Cu bulk, sized 15 mm × 10 mm, located in the powder capsule. The density was confirmed as about 97% of theoretical density, and hardness was about 75–80 Hv. The middle position of the compact was affected by the fast and high shock pressure, and a small-sized crack was observed. Because graphite powder is a very difficult-to-consolidate material due to its high melting point and low coefficient thermal expansion, interparticle melting between the graphite and Cu powder particles did not occur. The Cu powder particles were bonded only with each other, making graphite powder particles easily separable; thus, there was only weak surface bonding between both types of powder particles. Some voids were observed in most of the surface areas as shown in

Figure 8. Here, we suggest that a higher shock pressure of over 15 GPa is required to consolidate graphite powders because of high compressive strength and low thermal expansion coefficient.

4. Conclusions

To obtain a large-sized bulk sample, we designed a large-sized, convex type water container and investigated the magnitude, distribution and propagation behavior of shock pressure impacting powders numerically and experimentally. It was confirmed that reflected waves are generated, which converge and overtake the underwater shock wave. The magnitude of shock pressure at the central and 7.5 mm positions was almost identical at 12.8 GPa, whereas the pressure near the wall was lower because the reflected waves move to the central axis and converge. The experimental result of shock pressure was about 11.5 GPa. In consolidation of graphite doped Cu powders, weak surface bonding between both graphite and Cu powder particles was confirmed, and a small crack was observed in the middle position of the compact because of fast and high shock pressure; it is thus considered that a high shock pressure of over 15 GPa is required to consolidate graphite powders. We successfully obtained a shock-consolidated

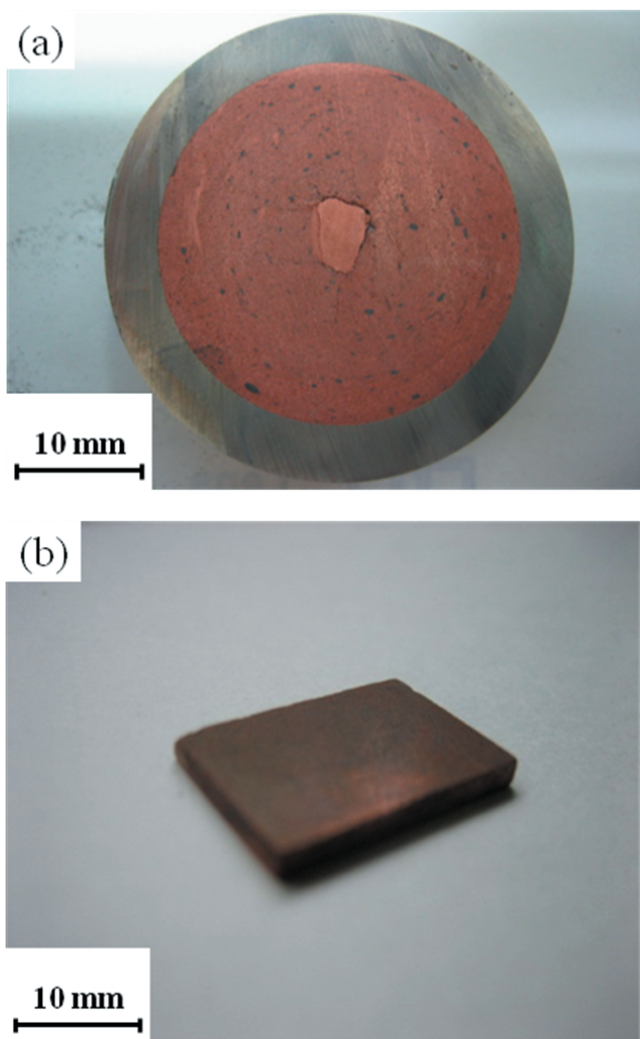


Figure 7 Photograph of (a) shock-consolidated graphite doped Cu bulk in the powder capsule and (b) processed graphite doped Cu bulk with the size of 15 mm \times 10 mm.

graphite doped Cu bulk with the large size of 15 mm \times 10 mm. However, more study is needed on consolidation problems related to materials with a high compressive

strength and low thermal expansion coefficient.

References

- 1) S. Ando, Y. Mine, K. Takashima, S. Itoh, and H. Tonda. Explosive compaction of Nd-Fe-B powder. *J Mater Process Technol* 85, 142 (1999).
- 2) Z. Q. Jin, K. H. Chen, J. Li, H. Zeng, S. F. Cheng, J. P. Liu, Z. L. Wang, and N. N. Thadhani. Shock compression response of magnetic nanocomposite powders. *Acta Mater* 52, 2147 (2004).
- 3) Y. Kim, T. Ueda, K. Hokamoto, and S. Itoh. Electric and microstructural characteristics of bulk ZnO fabricated by underwater shock compaction. *Ceram Inter* 35, 3247 (2009).
- 4) K. Raghukandan, K. Hokamoto, J. S. Lee, A. Chiba, B. C. Pai. An investigation on underwater shock consolidated carbon fiber reinforced Al composites. *J Mater Process Technol* 134, 329 (2003).
- 5) A. Chiba, M. Fujita, M. Nishida, K. Imamura, and R. Tomoshige. Underwater-Shock Consolidation of Difficult-to-consolidate Powders. In: Meyers MA, Murr LE, Staudhammer KP, editors. *Shock-wave and high-strain-rate phenomena in materials*, New York: Marcel Dekker; p. 415 (1992).
- 6) P. K. Rohatgi, S. Ray, and Y. Liu. Tribological properties of metal matrix graphite particle composites. *Int Mater Rev* 37, 129 (1992).
- 7) J. Kováčik, Š. Emmer, J. Bielek, and L. Keleši. Effect of composition on friction coefficient of Cu-graphite composites. *Wear* 265, 417 (2008).
- 8) A. Nakamura, and T. Mashimo. Calibration Experiments of a Thin Manganin Gauge for Shock-Wave measurement in Solids: Measurements of Shock-Stress History in Alumina. *J. Appl. Phys.* 32, 4785 (1993).
- 9) S. Itoh, S. Kubota, S. Kira, A. Nagano, and M. Fujita. On Underwater shock wave generated by underwater explosion of high explosives (1). *J Jap Exp losives Soc* 55, 202 (1994).
- 10) S. Itoh, S. Kubota, S. Nagano, and M. Fujita. On generation of ultra-high pressure by converging of underwater shock waves. *J Pressure Vessel Technol* 120, 51 (1998).

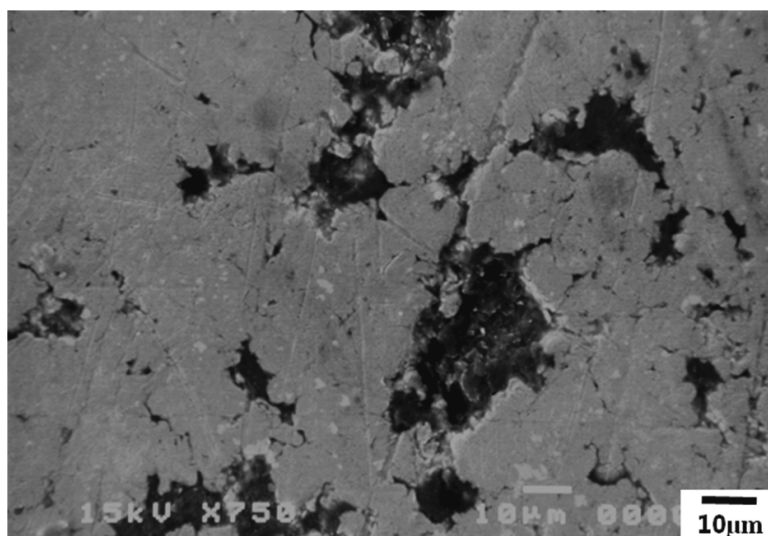


Figure 8 Microstructure of shock-consolidated graphite doped Cu bulk.